FTIR spectroscopic study on nickel(II)-exchanged sulfated alumina: nature of the active sites in the catalytic oligomerization of ethene

Anatoli A. Davydov [a,*], Margarita Kantcheva [b], and Marina L. Chepotko [a]

[a] Xenon C&P Co., 1305 W 113 Street, Jenks, OK 74037, USA
[b] Department of Chemistry, Bilkent University, 06533 Bilkent, Ankara, Turkey

Received 11 April 2002; accepted 1 June 2002

The nature of the active sites in nickel(II)-exchanged sulfated alumina in the reaction of ethene oligomerization has been studied by means of FTIR spectroscopy of adsorbed CO. It has been established that isolated nickel(I) species are the active sites in this process. These sites are formed by a reduction process, in which protonic centers are involved. The latter are due to the presence of covalently-bonded sulfate ions on the catalyst surface.

KEY WORDS: dimerization; ethene; nickel-exchanged sulfated alumina; nature of active sites; FTIR study.

1. Introduction

Materials such as nickel oxide and nickel salts supported on silica and/or alumina have been used as catalysts for dimerization and oligomerization of olefins. In general, nickel-exchanged silica–alumina possesses high activity and selectivity for conversion of ethene to C_{10+} products [1,2], whereas nickel–alumina catalysts modified by sulfate ions perform well in the synthesis of dimers of ethene and propene [3–8].

The viewpoints regarding the nature of the active sites in nickel-based oligomerization catalysts are controversial. Yashima *et al.* [9] concluded that zero-valence nickel that is highly dispersed in the zeolite support is the active site. Other authors [10] suggested Ni^{2+} ions in a high coordinative unsaturation. There are strong arguments supporting the opinion that the active sites responsible for ethene oligomerization consist of Ni^{+} ions. It has been found that monovalent nickel can be produced from well-dispersed nickel(II) by reduction with alkene, mild reduction with hydrogen or photoreduction at 77 K [5,6,11–16], and the reduced catalysts are more active in the olefin oligomerization. Cai *et al.* [5] observed an induction period of ethene oligomerization over $NiSO_4/Al_2O_3$ catalyst heated in an oxygen atmosphere, but no induction period was observed with catalyst heated under vacuum. This also appears to support the importance of Ni^{+} ions as active sites since the induction period can result from the reduction of Ni(II) to Ni(I). The ESR and FTIR data showed that this catalytic system contains Ni(I) formed by partial reduction of Ni(II) with a low-carbon number olefin (ethene or propene). Based on these experimental facts, the Ni(I) species in conjunction with the strong acid centers of the support have been suggested as active sites for ethene dimerization [5,6].

The activity and selectivity of these catalysts is usually affected by strong adsorption of the products and by isomerization and co-polymerization of the olefins into branched products [17,18]. With the majority of the catalysts described in the literature, the conversion of ethene is observed to decrease rapidly with the reaction time due to deactivation of the catalysts and steady state has not been generally reached. However, under high pressures and temperatures between 393 and 453 K [1] or using a slurry reactor [2], amorphous and mesoporous nickel-exchanged silica–alumina catalysts showed high stabilities and high selectivities to C_{10+} products. The successful application of a slurry reactor has been reported earlier by Zhang *et al.* [7,8]. They observed during the oligomerization of ethene a steady-state performance of a catalyst prepared by ion exchange of nickel amine complex with sulfated nonporous fumed alumina (ALON^{TM}, Cabot Corporation). The reaction was carried out in a well-agitated, gas–liquid–solid slurry reactor under near-atmospheric pressure and a temperature of 298 K and below. Under these conditions, no deactivation of the catalyst has been observed. With a reaction temperature in the range tested, 279–298 K, 100% conversion of ethene and selectivities of 89 and 11% to 1-butene and 1-hexene, respectively, have been observed.

In the present paper, details about the nature of the active sites of nickel-exchanged sulfated alumina used by Zhang *et al.* [7,8] as a catalyst for the oligomerization

* To whom correspondence should be addressed.
E-mail: anatolid@hotmail.com

1011-372X/02/1000-0097/0

of ethene are reported. In order to investigate the role of the methods of catalyst preparation on the dispersion of nickel and its stabilization in various oxidation states, materials obtained by impregnation of γ-Al_2O_3 with aqueous solutions of nickel(II) nitrate and sulfate have also been used. For identification of the oxidation state of the supported nickel, FTIR spectroscopy of adsorbed CO has been employed. It is well known that the ν(CO) stretching frequencies in carbonyl complexes with nickel ions in various oxidation states appear in different spectral regions [15,16,19–26]: below 2100 cm^{-1} for Ni(0), between 2120 and 2160 cm^{-1} for Ni(I) and above 2170 cm^{-1} for Ni(II). The adsorption of CO has been performed on freshly activated samples and after interaction with ethene. The poisoning effect of CO on the interaction of ethene with the catalysts has been investigated as well.

2. Experimental

2.1. Catalyst preparation

The support used was ultra-fine non-porous γ-alumina support (ALON). The Ni(II) ions were added by either impregnation or ion-exchange methods. The BET surface areas and the content of the active components of the materials studied are given in table 1.

2.1.1. Impregnation method

The catalyst with nominal nickel content of 3.5 wt% was prepared by impregnation with an aqueous solution of $NiSO_4 \cdot 6H_2O$. This sample is denoted by 3.5NAS. The sulfate-modified support was obtained by impregnation with an aqueous solution of $(NH_4)_2SO_4$ (Fisher). The amount of sulfate ions in the modified support (notation 5.7AS) is equal to that of the 3.5NAS sample (5.7 wt% of SO_4^{2-} ions).

A sample containing 3.5 wt% of nickel on pure ALON was also prepared by impregnation with an aqueous solution of $Ni(NO_3)_2 \cdot 6H_2O$ (notation 3.5NA). The impregnated samples were dried at 393 K and calcined at 773 K for 4 h.

Table 1
BET surface areas and composition of the catalysts studied.

Catalyst notation	BET area (m^2/g)	Nickel content (wt%)	SO_4^{2-} content (wt%)
γ-Al_2O_3	102	–	–
5.7AS	101	–	5.7
3.5NA	113	3.5	–
3.5NAS	112	3.5	5.7
0.9NAS-Ex	109	0.9	5.7
1.7NAS-Ex	111	1.7	5.0

2.1.2. Ion-exchange method

A nickel amine complex was prepared by dissolving $Ni(NO_3)_2 \cdot 6H_2O$ in an aqueous solution of ammonia (Fisher) at pH 11. The dry sulfated alumina (5.7AS) was added to the nickel complex solution for ion exchange. After agitation for 6 or 12 h, the solid phase was filtered from the suspension and washed with deionized water, dried at 393 K, washed again and dried at 393 K for 4 h. Final calcinations at 773 K for 4 h completed the procedure for the preparation of the ion-exchanged sample. The nickel content was determined by flame atomic absorption spectrometry at the respective resonance wavelength. The sample obtained by contact of the nickel complex solution with the sulfated support for 6 h contained 0.9 wt% of nickel. This sample was denoted by 0.9NAS-Ex. The ion-exchange procedure performed for 12 h led to higher loading of nickel (1.7 wt%) and this material was denoted by 1.7NAS-Ex. The prolonged contact of the sulfated support with the basic nickel solution caused some leaching of sulfate ions from the modified alumina. The amount of sulfated ions lost was determined by precipitation as barium sulfate. The precipitate was dissolved in an excess of standard EDTA solution and the excess of EDTA was back-titrated with standard magnesium solution using solochrome black as indicator. The amount of sulfate ions in the 1.7NAS-Ex catalyst was 5 wt%.

2.2. FTIR measurements

The samples, pressed into thin pellets, were heated under vacuum (1.33×10^3 Pa) at 773 K for 1 h followed by different activation procedures: (i) thermoactivation—calcination under 13.3 kPa of oxygen at 773 K with subsequent evacuation for 2 h at the same temperature; (ii) treatment in oxygen atmosphere—heating in oxygen (13.3 kPa) for 1 h at 773 K, followed by cooling down to room temperature in an oxygen atmosphere and evacuation for 1 h at the latter temperature (oxidized sample); (iii) reduction of the oxidized sample at 473, 573, 673 and 773 K, respectively, in CO (2.67 kPa) for 30 min, followed by evacuation for 1 h at the corresponding reduction temperature. The pure alumina and the 5.7AS sample were thermoactivated.

The dimerization of ethene was performed under static conditions in the FTIR cell. The spectra were taken *in situ* by a Nicolet FTIR spectrometer model 730 (160 scans). The resolution was 2 cm^{-1}.

Gases with high purity (O_2, CO and C_2H_4) were purchased from Matheson.

3. Results

3.1. Al_2O_3 and 5.7AS sample

The spectrum of adsorbed CO on the activated pure alumina (ALON) is characterized by a carbonyl

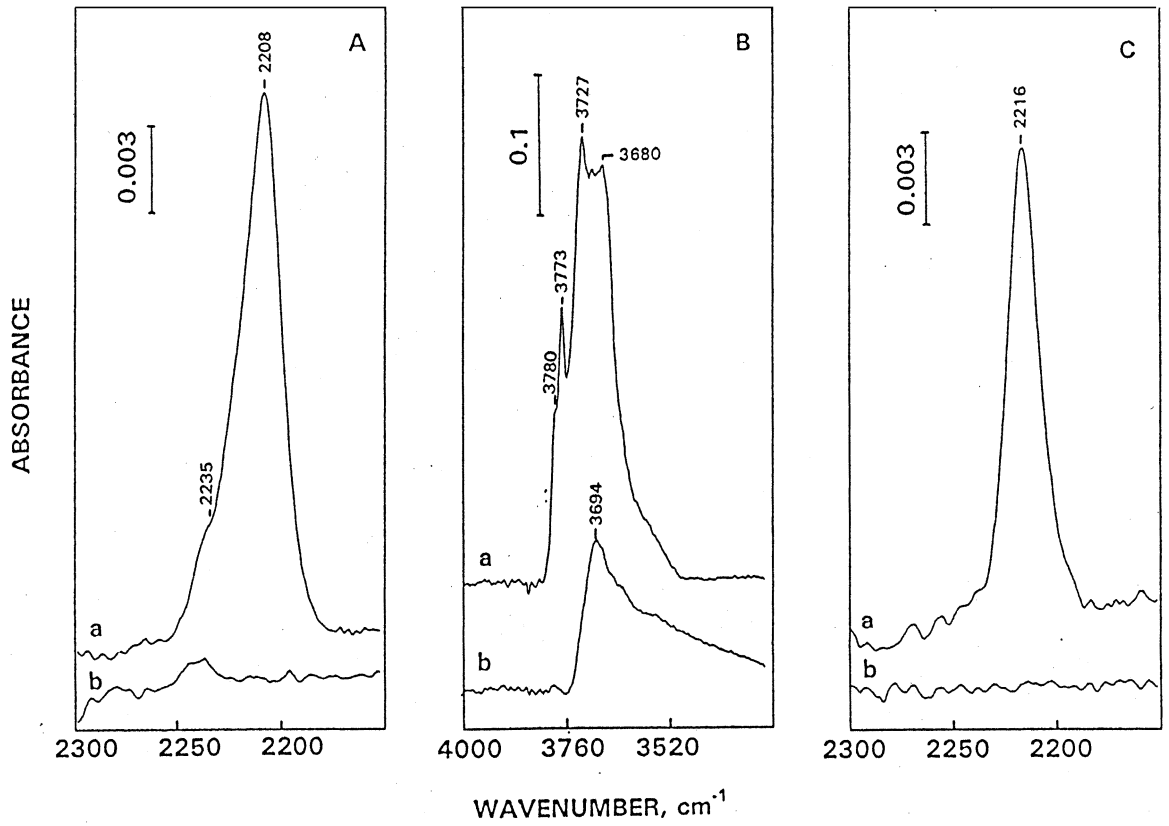

Figure 1. (A) FTIR spectra of (a) adsorbed CO (1.33 kPa, room temperature) on alumina (ALON) thermoactivated at 773 K and (b) after evacuation for 2 min at room temperature; (B) FTIR spectra in the OH stretching region taken after thermoactivation at 773 K of (a) alumina (ALON) and (b) sample 5.7AS; (C) FTIR spectra of (a) adsorbed CO (1.33 kPa, room temperature) on sample 5.7AS thermoactivated at 773 K and (b) after evacuation for 2 min at room temperature.

band at 2208 cm^{-1} with a shoulder at 2235 cm^{-1} (figure 1(A)). These bands are observed on γ-Al_2O_3 [21,27] and correspond to CO adsorbed on coordinatively unsaturated (cus) aluminum ions in octahedral and tetrahedral coordination, respectively. In the OH stretching region, isolated hydroxyl groups with frequencies at 3780, 3773, 3727, 3704 and 3680 cm^{-1}, typical for transition aluminas [27], were observed (figure 1(B), spectrum (a)). The modification of the support with SO_4^{2-} ions leads to disappearance of the OH groups with bands between 3780 and 3700 cm^{-1} (figure 1(B), spectrum (b)). This indicates that part of the OH groups was replaced by sulfate ions. On the 5.7AS sample, isolated OH groups with absorption at 3694 cm^{-1} are observed. The low-frequency shoulder to this band indicates that hydrogen-bonded OH groups are present on the catalyst surface. The adsorption of CO on the latter sample reveals the existence of cus Al^{3+} ions, which are characterized by a single carbonyl band at 2216 cm^{-1} (figure 1(C)). Obviously, there are sulfate groups coordinated to the stronger electron acceptor sites of the support, making them inaccessible to CO adsorption. The carbonyl species observed are not stable and disappear after evacuation for 2 min at room temperature.

3.2. 3.5NA sample

The adsorption of CO on the thermoactivated 3.5NA sample results in the appearance of several bands in the carbonyl region (figure 2(A), spectrum (a)). The band at 2187 cm^{-1} is characteristic for Ni^{2+}–CO species [15,16,19–26]. The weak absorption at approximately 2230 cm^{-1} and the high-frequency shoulder of the Ni^{2+}–CO band indicate that some cus Al^{3+} ions of the support are still present after the deposition of the nickel ions. These carbonyl bands are observed with very low intensity after evacuation for 15 min at room temperature (figure 2(A), spectrum (b)). The broad and weak absorption centered at about 2127 cm^{-1} and detected only in CO atmosphere is assigned to the ν(CO) stretching mode of CO linearly bonded to Ni^{+} ions [15,16,19–25]. However, a contribution to this absorption band from CO weakly interacting with the hydroxyl groups cannot be excluded. Indeed, a perturbation of the bands corresponding to the OH stretching vibration upon CO adsorption is detected too (the spectra are not shown). The absorption at 2092 cm^{-1}, which is very resistant to evacuation, is due to $Ni^{\delta+}$–CO species [19–25]. The band at 1830 cm^{-1} is assigned to bridge carbonyls formed on metallic nickel [15,19–25].

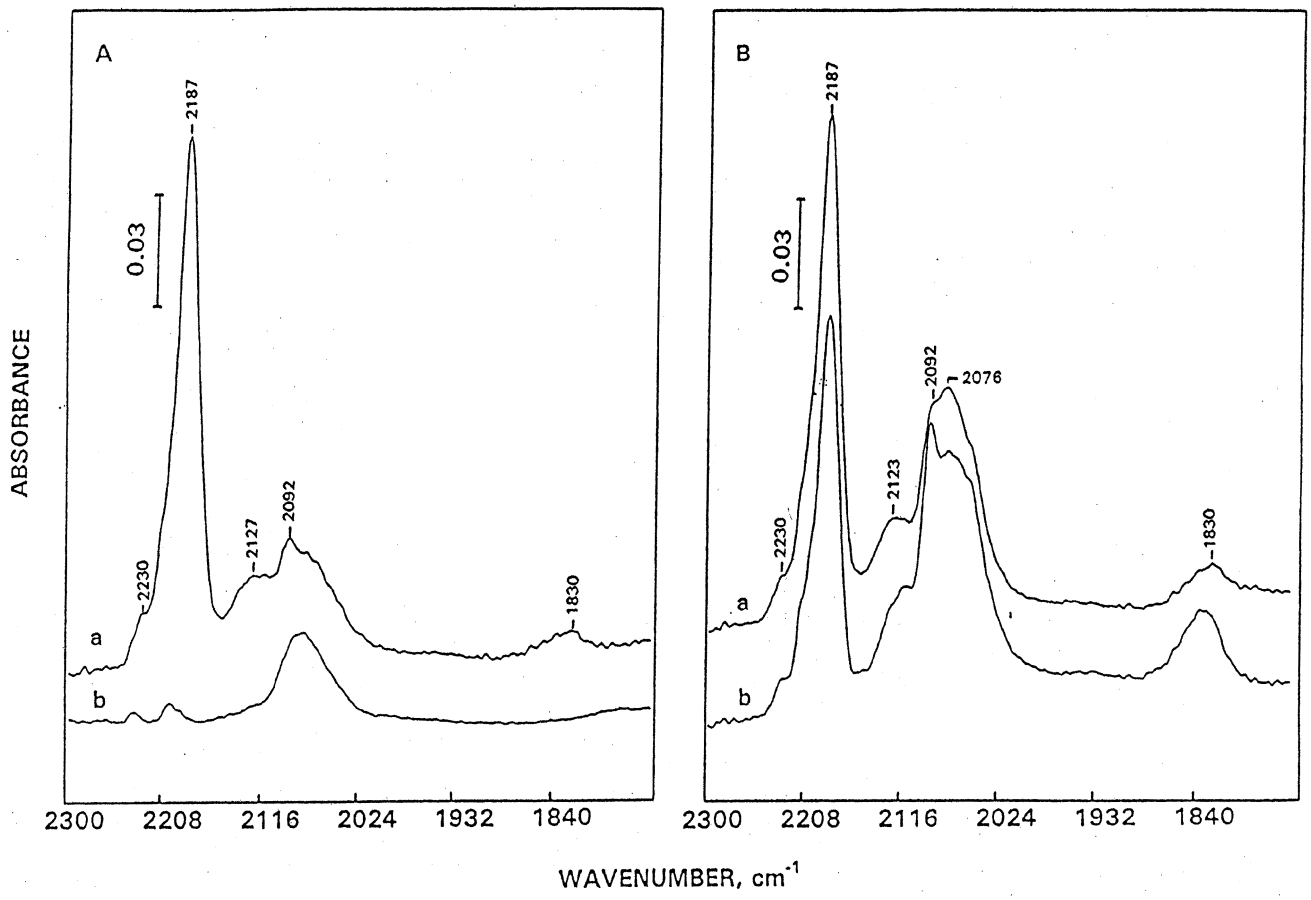

Figure 2. (A) FTIR spectra of (a) adsorbed CO (1.33 kPa, room temperature) on sample 3.5NA thermoactivated at 773 K and (b) after evacuation for 15 min at room temperature. (B) FTIR spectra of adsorbed CO (1.33 kPa, room temperature) on sample 3.5NA after reduction with 2.67 kPa of CO for 30 min at (a) 573 K and (b) 673 K. The reduction of the sample was followed by evacuation for 1 h at the corresponding reduction temperature.

The reduction of the sample with CO at 573 and 673 K leads to a decrease in the intensity of the Ni^{2+}–CO band and to a noticeable increase in the amount of the $Ni^{\delta+}$–CO species (figure 2(B)). It should be pointed out that the spectrum of isolated hydroxyl groups of the 3.5NA sample does not differ from that of the pure support.

3.3. 3.5NAS sample

The spectra of adsorbed CO on the thermoactivated 3.5NAS sample are shown in figure 3(A). The absorption at 2206 cm^{-1} (spectrum (a)) is assigned to Ni^{2+}–CO species. The position of this band compared with the sulfate-free sample is blue-shifted by approximately 20 cm^{-1}. In addition, these species display higher stability than those on the 3.5NA sample and are detected in the spectrum after evacuation for 15 min at room temperature (figure 2(B), spectrum (b)). No absorption bands which can be assigned to Al^{3+}–CO carbonyls are observed. This indicates that there are no cus Al^{3+} ions exposed on the catalyst surface detectable by CO adsorption at room temperature. The spectrum in the OH stretching region is identical to that shown for the 5.7AS sample.

The influence of the activation procedure on the oxidation state of nickel is studied by adsorption of CO and the results are shown in figure 3(B). The adsorption of 2.67 kPa of CO on the oxidized sample gives rise to the band at 2206 cm^{-1}, which has been attributed already to Ni^{2+}–CO carbonyls. The intensity of this band is weaker compared with that of the thermoactivated sample (figure 3(A), spectrum (a)), which indicates lower amount of cus Ni^{2+} ions on the surface of the oxidized sample. The subsequent reduction of the sample with CO at 473 and 573 K (figure 3(B), spectra (b) and (c)) leads to a slight increase in the intensity of the carbonyl band at 2206 cm^{-1}. In all these cases, weak absorption bands at about 2150 and 2100 cm^{-1} are observed. After reduction at 673 K, noticeable changes in the spectrum of adsorbed CO are detected (figure 3(B), spectrum (d)). The intensity of the bands at 2145 and 2100 cm^{-1} has increased, whereas that for the Ni^{2+}–CO species at 2206 cm^{-1} has decreased slightly. A new band at 1900 cm^{-1} has appeared. The pair of bands at 2145 and 2100 cm^{-1} is assigned to symmetric and asymmetric ν(CO) stretching modes, respectively, of $Ni^{+}(CO)_2$ species, whereas the broad absorption at 1900 cm^{-1} is attributed to bridged Ni–(CO)–Ni complexes [15,19–25]. The assignment of

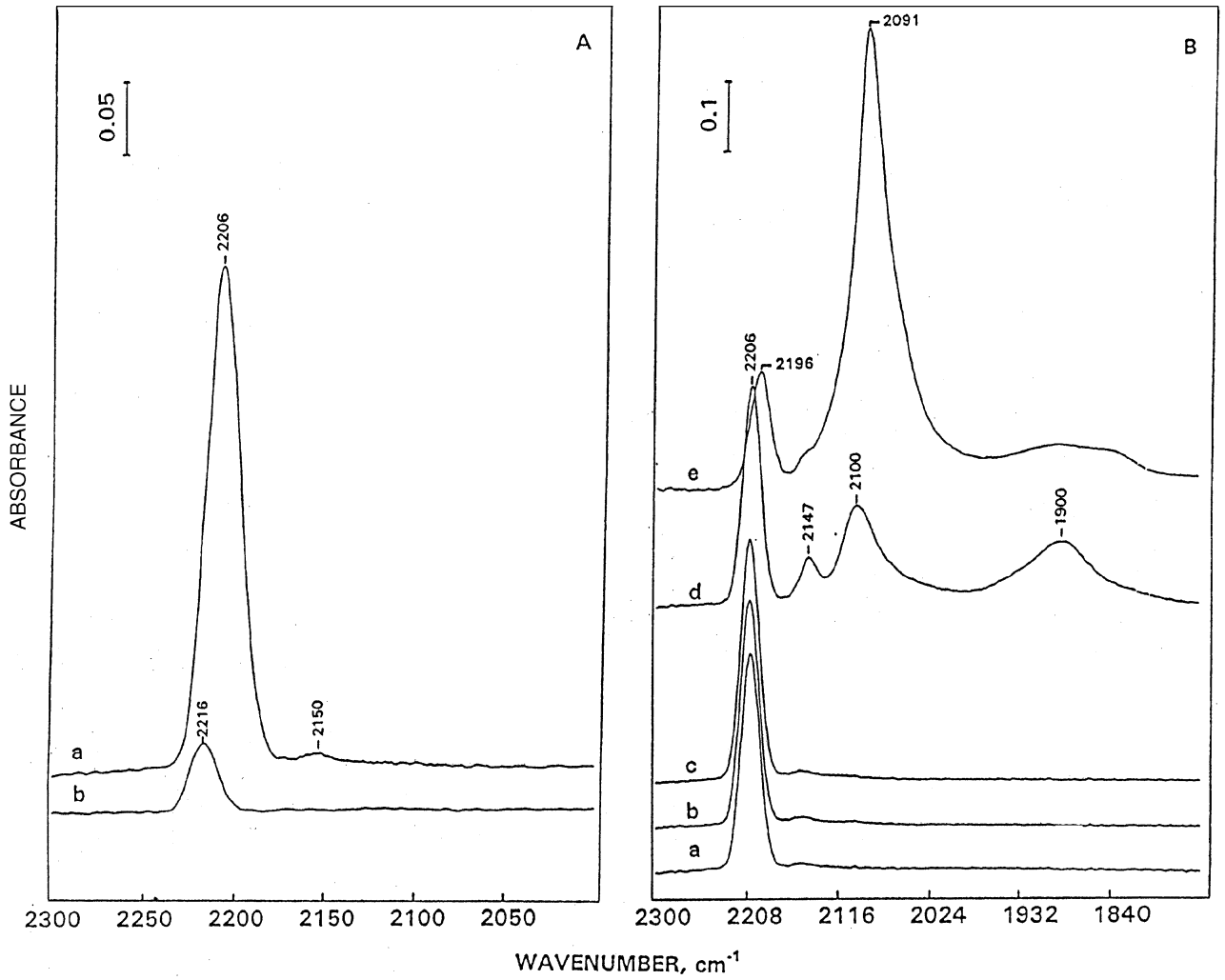

Figure 3. (A) FTIR spectra of (a) adsorbed CO (2.67 kPa, room temperature) on sample 3.5NAS thermoactvated at 773 K and (b) after evacuation for 15 min at room temperature. (B) FTIR spectra of adsorbed CO (2.67 kPa, room temperature) on 3.5NAS (a) after oxidizing activation procedure and after reduction with 2.67 kPa of CO for 30 min at (b) 473 K; (c) 573 K; (d) 673 K; and (e) 773 K. The reduction of the sample was followed by evacuation for 1 h at the corresponding reduction temperature.

the bands at 2145 and 2100 cm^{-1} to dicarbonyls coordinated to Ni^{+} sites is based on the literature data*. Since their behavior during the variation of CO pressure in our study has been similar to those observed by Che and coworkers [14(a)], the spectra are not shown. The increase in the pressure is accompanied by a proportional growth in the intensities of the bands at 2145 and 2100 cm^{-1}. This doublet is converted to a single band at 2118 cm^{-1} after the evacuation. Admission of CO restores the doublet. The position of the doublet [24], as well as the intensity ratio [23], is characteristic for dicarbonyl species formed in nickel mordenite [25], NiCaX [15] and Ni/Al_2O_3 [22]. The transformation of the dicarbonyl into a monocarbonyl, as reflected by the conversion of the doublet into a single band at lower CO pressure, is obviously reversible. It should be noted that the IR spectra reported by Cai *et al.* [5] are not due to Ni^{+}–CO complexes, as these authors suggested. The absorption bands at 2170 and 2120 cm^{-1} reported by them fall in the region of the P and Q rotation branches of gaseous CO. These absorption bands appear in the spectra of adsorbed CO when high pressures are used. The observed increase in the intensities of the bands at 2170 and 2120 cm^{-1} with increase in the CO pressure (up to 40 kPa), reported in references [5] and [6], supports this conclusion. Such a possibility for misinterpretation of the IR spectra of adsorbed CO has been discussed elsewhere [28].

* At present, basically due to the studies of Che *et al.* [14] (also, see [19–22]), there is clear evidence for the assignment of these absorption bands to the $Ni^{1+}(CO)_2$ complex. Such studies have been started by ESR and UV–vis investigations of the Ni^{1+} ions in zeolites with an identification of the complex formed between nickel ions in such oxidation states with CO molecules by means of IRS [15,19,23]. Then, the direct proofs for the assignments of the same bands to $Ni^{1+}(CO)_2$ have been obtained for the nickel-exchanged silica [14], reduced either by mild thermal reduction in hydrogen or by photoreduction in hydrogen at 77 K (for preferentially stabilizing the Ni^{1+} oxidation state), by means of the analysis of ESR spectra of Ni^{1+} ions both before and after their interaction with CO and FTIR spectra of adsorbed CO, including those at the change of partial pressure of adsorbed CO, and using the mixture of ^{12}CO and ^{13}CO [14(c)].

Upon raising the reduction temperature up to 773 K a further decrease in the intensity of the Ni^{2+}–CO band (shifted to 2196 cm^{-1}) and a very strong increase in the intensity of the band at 2091 cm^{-1} corresponding to $Ni^{\delta+}$–CO species are observed (figure 3(B), spectrum (e)). The presence of Ni^{+} ions is judged by the shoulder at approximately 2150 cm^{-1} of the $Ni^{\delta+}$–CO band. The formation of the $Ni(CO)_4$ complex on investigated samples can be excluded since the intense band at 2040–2060 cm^{-1} characteristic for this complex has not been observed.

It is of interest to test the initial activity of the catalyst 3.5NAS toward ethene dimerization. Figure 4 represents the consumption of ethene (expressed in mmol per gram catalyst) on thermoactivated, reduced and oxidized catalyst, respectively. The thermoactivation and reduction of the catalyst up to 673 K leads to comparable initial activity. Under these conditions, according to the spectra of adsorbed CO (figure 3), the catalyst surface is characterized by co-existence of Ni^{+} ions with high coordinative unsaturation and Ni^{2+} ions in higher surface concentration. It should be pointed out that detection of minor amounts of Ni^{+} ions is possible because of the much higher molar absorptivity of the Ni^{+}–CO compared with that of the Ni^{2+}–CO species.

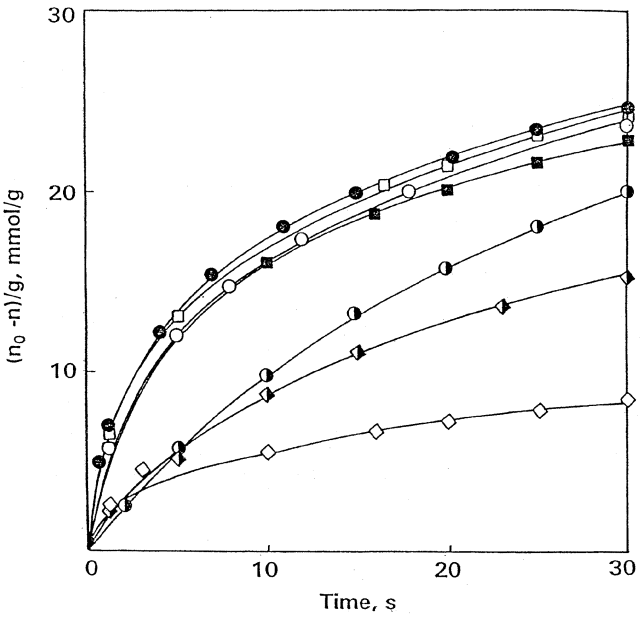

Figure 4. Consumption of ethene (initial pressure of 1.67 kPa) with the time during the oligomerization at room temperature in the presence of sample 5.7AS thermoactivated at 773 K (◇) and sample 3.5NAS after oxidizing activation procedure (◈), thermoactivation at 773 K (◑) and reduction with 2.67 kPa CO for 30 min at 473 K (○); 573 K (□); 673 K (●); and 773 K (■).

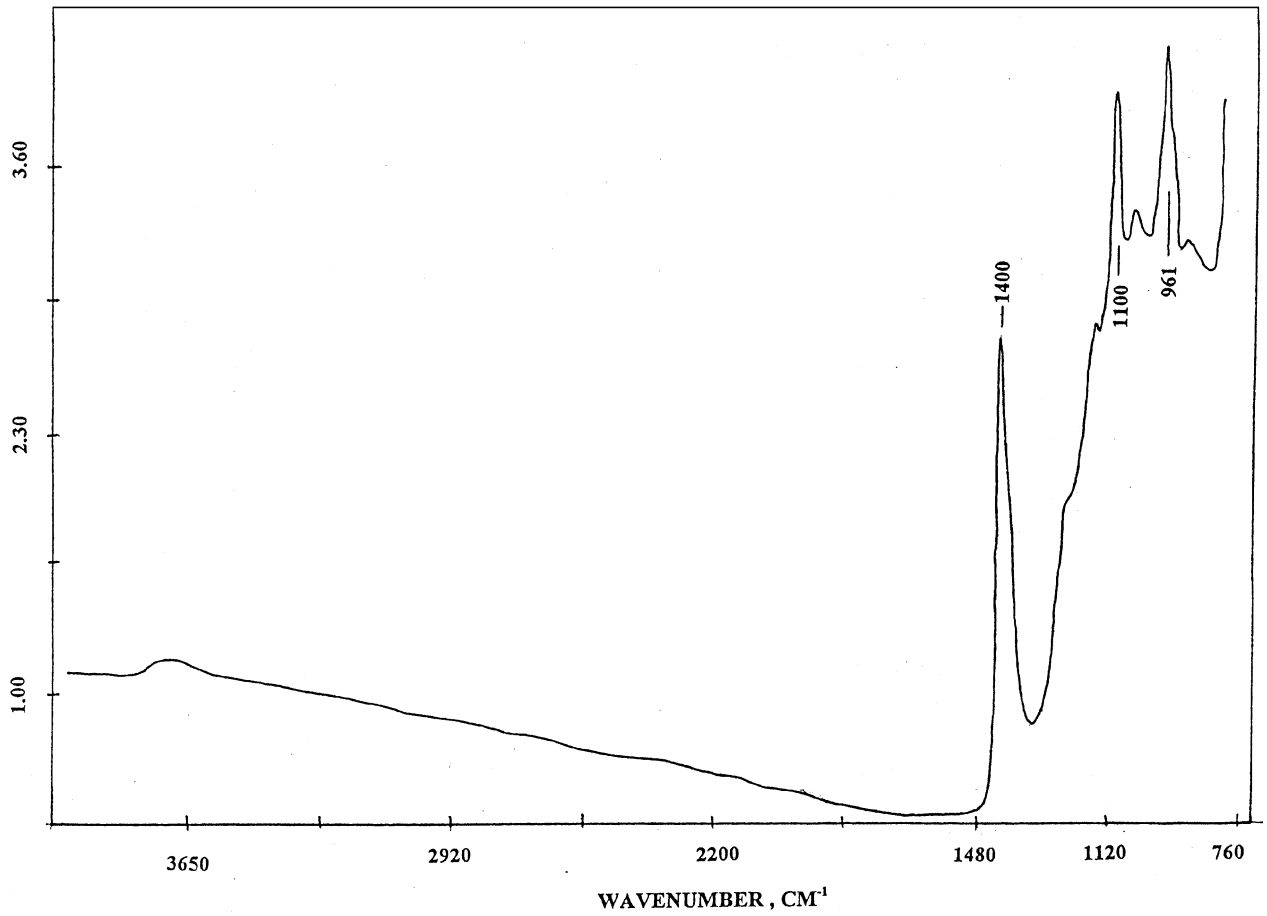

Figure 5. FTIR spectrum of the 1.7NAS sample after treatment at 773 K for 2 h under vacuum.

This difference is due to a larger contribution of the π component in the Ni^{+}–CO bond [21]. This allows detection of Ni^{+} sites in the IR spectra even at concentrations substantially lower than those of Ni^{2+} ions.

The activity of the oxidized catalyst and the sulfated alumina are close, which indicates that the catalytic effect in this case is due mainly to the modified support. In all cases deactivation kinetics is observed, caused by the strong adsorption of the reaction products under the experimental conditions (low pressure and absence of solvent). The spectra of the adsorbed products correspond to butenes.

3.4. 1.7NAS-Ex sample

Figure 5 displays the FTIR spectrum of the thermoactivated 1.7NAS-Ex sample. According to the literature data [29–31], the band at 1400 cm^{-1} is characteristic for the ν(S=O) vibration of covalent surface sulfates, whereas the bands at 1100 and 961 cm^{-1} are typical for the ν(S–O) vibrations. These compounds have C_s or C_{2v} symmetry as in bidentate sulfate species, but the S–O bond order is close to 2, *i.e.*, the SO_2 fragment of these species should be considered as quasi-isolated, in contrast to the ionic sulfates, in which the cation coordinates the sulfate groups as a whole. The weaker bands at 1156, 1040 and 904 cm^{-1} can be attributed to more ionic sulfate species [29–31].

It is known that the addition of sulfate ions to the surface of alumina results in enhanced Lewis and Brønsted acidity [32]. Figure 6 shows the effect of the activation temperature on the development of Brønsted acid sites (measured by adsorption of ammonia) in the catalyst 1.7NAS-Ex. The changes in the intensity of the band at 1440 cm^{-1} due to the $\delta_s(NH_4^+)$ mode indicate that the sample thermoactivated at 773 K possesses a considerably larger amount of Brønsted acid sites than that treated at 473 K. It should be noted that at temperatures of thermo-activation higher than 773 K, the concentration of the protonic sites on the 1.7NAS-Ex catalyst detectable by ammonia adsorption is very small, as has been observed in the case of pure alumina [21].

The adsorption of CO on the 1.7NAS-Ex sample (thermoactivated at 773 K) gives rise to a band at 2210 cm^{-1} characteristic for Ni^{2+}–CO (figure 7(A), spectrum (a)), which shifts to 2215–2217 cm^{-1} upon brief evacuation at room temperature (spectrum (b)). The single band at 2160 cm^{-1} reveals the presence of Ni^{+}–CO species. The carbonyls observed cannot be destroyed by evacuation (CO residual pressure of 1.33 Pa). No carbonyls corresponding to metallic nickel are detected.

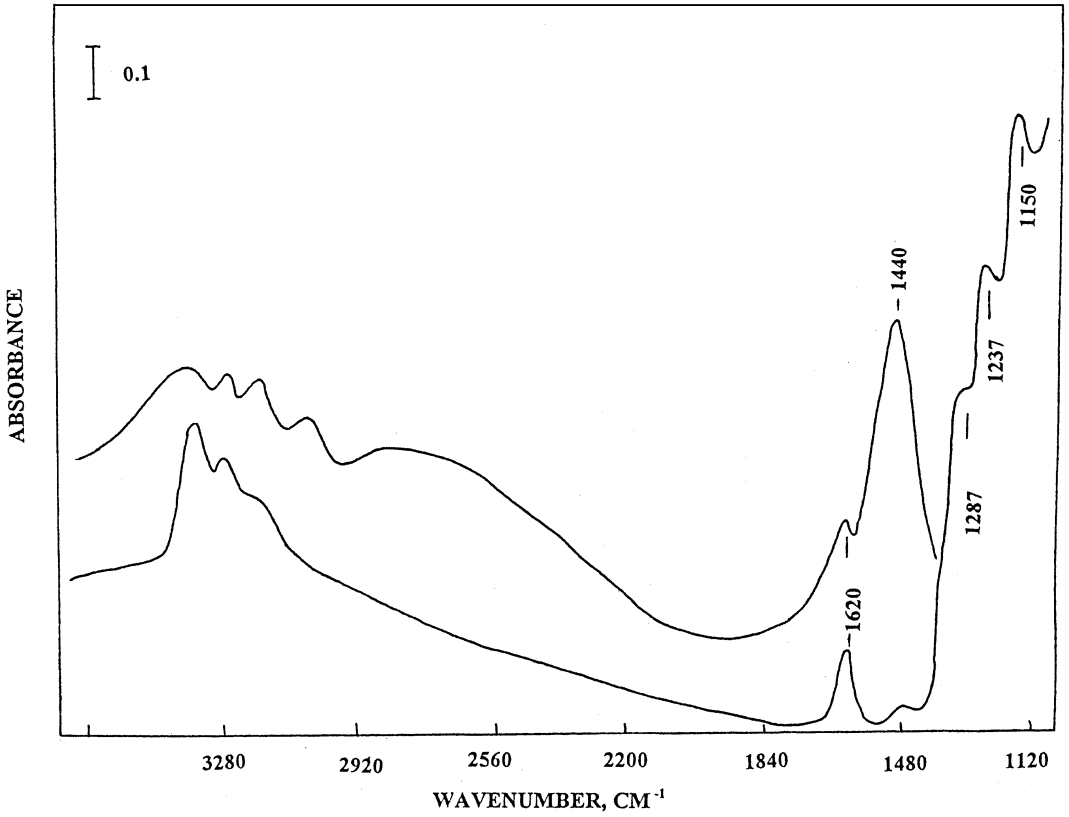

Figure 6. FTIR spectra of adsorbed NH_3 (1.33 kPa, room temperature) on sample 1.7NAS thermoactivated at (a) 473 K and (b) 773 K, followed by evacuation at room temperature for 10 min.

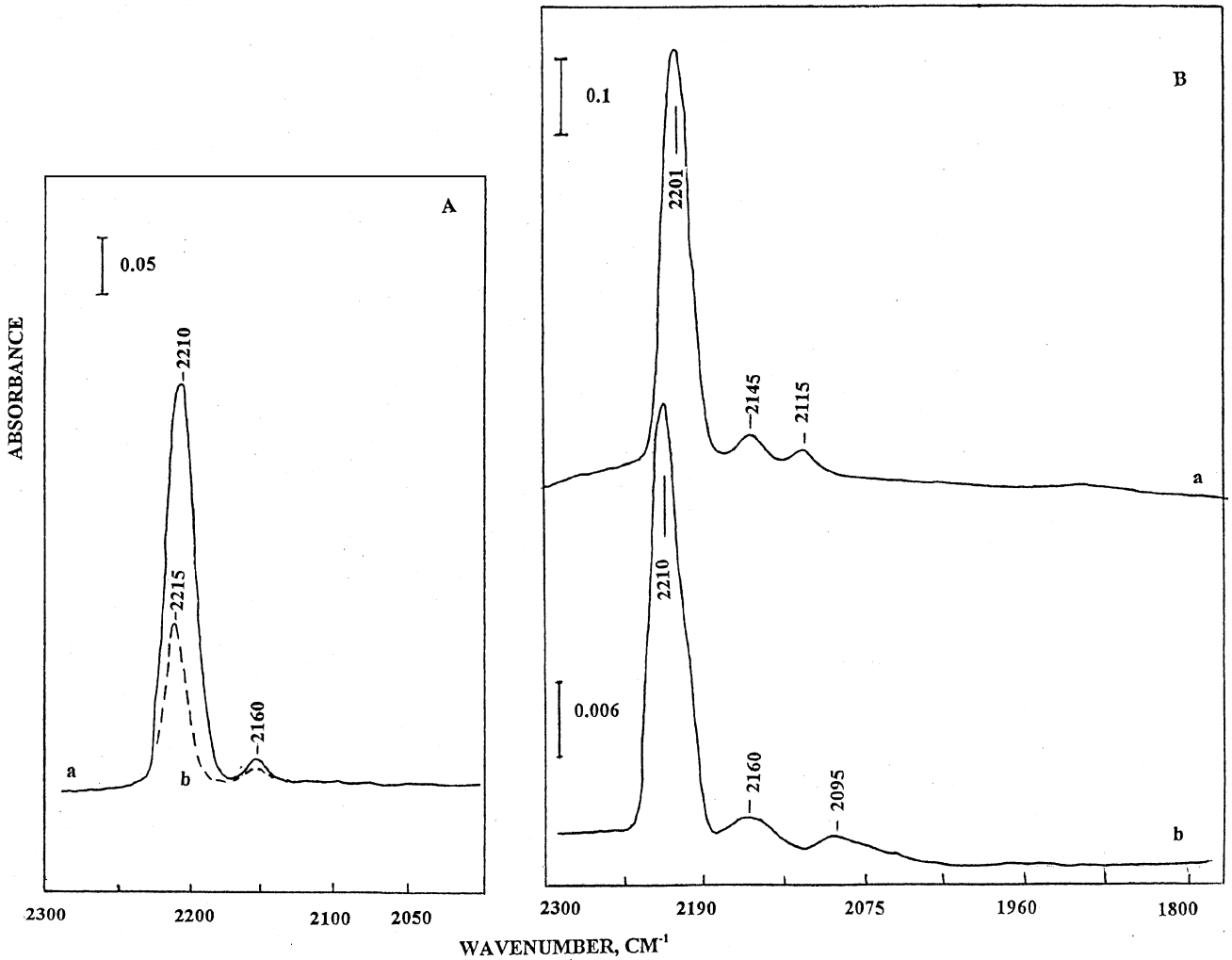

Figure 7. (A) FTIR spectra of (a) adsorbed CO (1.33 kPa, room temperature) on sample 1.7NAS thermoactivated at 773 K and (b) after evacuation for 1 min at room temperature. (B) FTIR spectra of adsorbed CO (1.33 kPa, room temperature) on 1.7NAS after reduction with 2.67 kPa of CO for 30 min at (a) 573 K and (b) after evacuation for 15 min at room temperature. The reduction of the sample was followed by evacuation for 1 h at the corresponding reduction temperature.

The reduction of the catalyst with CO at 573 K (figure 7(B), spectrum (a)) results in a substantial increase in the intensity of the band corresponding to Ni^{2+}–CO species compared with that in the case of the thermoactivated catalyst (figure 7(A), spectrum (a)). The same trend has been observed for the 3.5NAS catalyst. This behavior can be explained by the assumption that, after the reductive treatment, the amount of the cus Ni^{2+} has increased. The doublet at 2145 and 2115 cm^{-1} is assigned to the $Ni^{+}(CO)_2$ species (see above). The prolonged evacuation at room temperature (figure 7(B), spectrum (b)) leads to a considerable decrease in the intensity of the band due to Ni^{2+}–CO (shifted to 2210 cm^{-1}) and the disappearance of the band at 2115 cm^{-1}. The band at 2095 cm^{-1}, which is observed instead, is assigned to the $Ni^{\delta+}$–CO species. The absorption at 2160 cm^{-1} is attributed to a linear Ni^{+}–CO carbonyl. Obviously, the evacuation causes transformation of the dicarbonyls to monocarbonyls and disproportionation of Ni^{+} to Ni^{2+} ions and metallic nickel [15].

It is of importance to study the state of nickel ions on the catalyst surface after performing the reaction of oligomerization of ethene. The contact of the thermoactivated 1.7NAS-Ex catalyst with ethene (1.67 kPa) for 10 min at room temperature gives rise to bands at 2970, 2940 and 2875 cm^{-1} due to CH stretching vibrations of adsorbed butenes (the spectrum is not shown). After evacuation of the olefin for 10 min at room temperature, CO (1.33 kPa) has been introduced. The spectrum obtained in this way is shown in figure 8. This spectrum differs from the spectrum of adsorbed CO on freshly activated catalyst (figure 7(A), spectrum (a)) in the following: (i) the strong decrease in the intensity of the band at 2210 cm^{-1} due to Ni^{2+}–CO carbonyls; (ii) the absence of the band due to Ni^{+}–CO species (at 2160 cm^{-1}) and (iii) the appearance of a new band at 2095 cm^{-1} due to $Ni^{\delta+}$–CO species. This result indicates that partial reduction of the Ni^{2+} ions to low-valence nickel (Ni^{+} and $Ni^{\delta+}$) takes place. Probably, the ethene

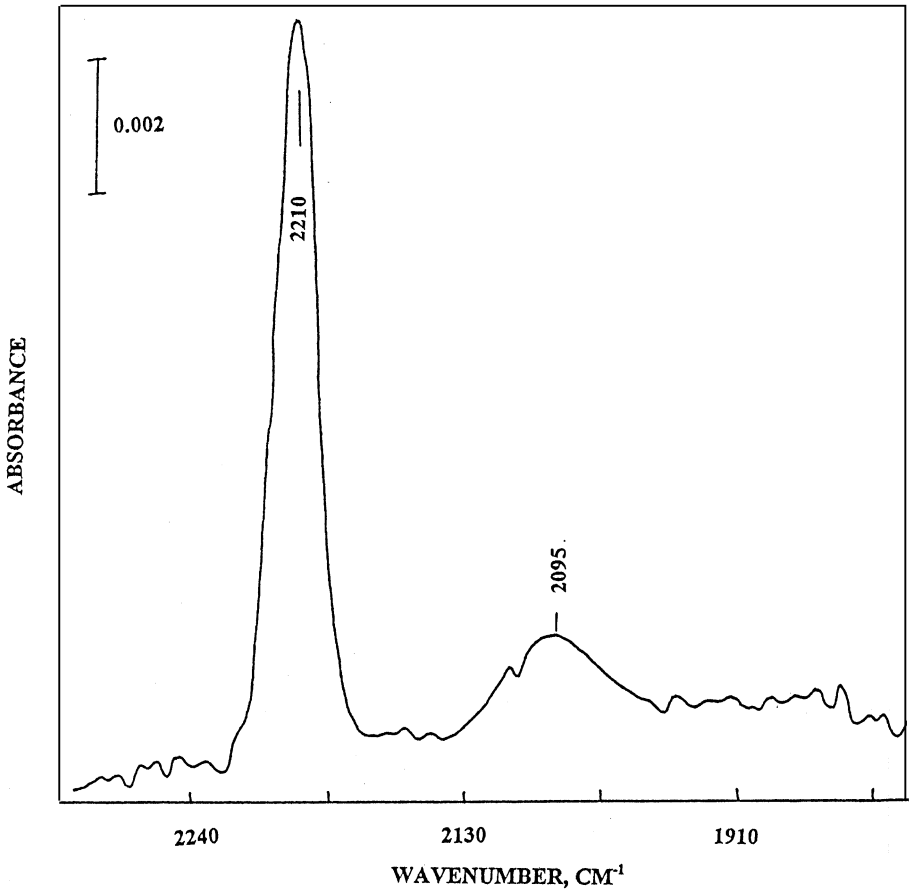

Figure 8. FTIR spectrum of adsorbed CO (1.33 kPa) on 1.7NAS sample after contact with 1.67 kPa of ethene at room temperature for 10 min followed by evacuation for 10 min at room temperature.

oligomers are adsorbed on the Ni^{+} sites and the latter cannot be detected by CO adsorption. The increase in the catalyst activity early in the process of ethene oligomerization accounts for the occurrence of this reduction process.

It should be pointed out that the intensities of the bands in the ν(CH) stretching region due to butenes produced by dimerization of ethene on the 1.7NAS-Ex catalyst activated by reduction with CO at 573 K is higher than those detected on the thermoactivated catalyst. If CO is introduced prior to the adsorption of ethene, these bands are absent. These experimental facts suggest that nickel species in low oxidation states play an important role in the activation of the olefin and its conversion to oligomers. The reduced nickel species form stable carbonyls upon CO adsorption that leads to loss of the catalyst activity.

3.5. 0.9NAS-Ex sample

It is known that the catalysts prepared by ion exchange are characterized by a more homogeneous distribution of the active components on the support. Figure 9 compares the activity of the sample 3.5NAS with that of the catalyst prepared by ion exchange of

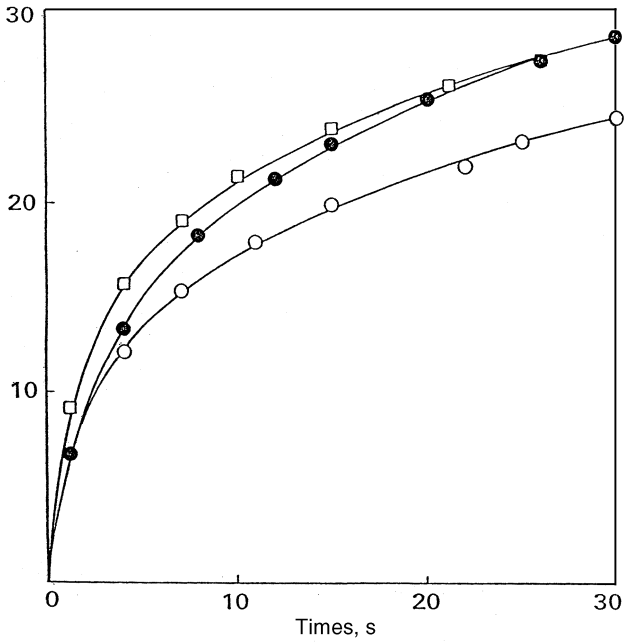

Figure 9. Consumption of ethene (initial pressure of 1.67 kPa) with time during the oligomerization at room temperature in the presence of the samples 0.9NAS-Ex (○), 3.5NAS (□) and the sample obtained by additional loading of Ni(II) (see the text) over the 0.9NAS sample (●). The catalysts are thermoactivated at 773 K.

Ni^{2+} ions (0.9NAS-Ex sample). It is visible that the latter catalyst is characterized by a higher activity, although it contains considerably lower amounts of supported nickel ions. The additional impregnation of the ion-exchanged catalyst with Ni^{2+} ions (from aqueous solution of nickel nitrate) in order to reach the total loading with nickel of 3.5 wt%, results in a catalyst with practically the same activity. This experimental fact leads to the conclusion that only nickel ions directly bonded to the support in conjunction with sulfate groups represent the active sites or their precursors in the reaction of ethene dimerization and that the saturation of the support surface with Ni^{2+} ions was reached during the ion exchange. On the 0.9NAS-Ex sample, after thermo activation, the appearance of Ni^{+} (absorption band at 2160 cm^{-1} due to linear Ni^{+}–CO species) together with Ni^{2+} ions (ν(CO) at 2217 cm^{-1}) is observed. No Ni^{0} species are detected even after reductive treatment.

4. Discussion

In general, there is agreement that the nickel ions on the surface of nickel-based catalysts are the active sites for ethene oligomerization. This is concluded from the fact that the amount of adsorbed ethene in the case of nickel-containing systems is more than the amount of ethene adsorbed by the support. The presence of sulfate ions has a significant effect on the activity of nickel–alumina catalysts, increasing it [7]. In addition, from the data on CO adsorption on NiO/Al_2O_3 (figure 2) and $NiSO_4/Al_2O_3$ catalysts (figure 3) it can be concluded that the sulfate ions diminish the reducibility of the Ni^{2+} ions. The thermoactivation and reduction of the 3.5NAS catalyst with CO at temperatures up to 573 K lead to the appearance of a small amount of Ni^{+} ions. The concentration of low-valence nickel increases at higher temperatures, and after reduction at 673 K considerable amounts of Ni^{+} and $Ni^{\delta+}$ are observed.

The data on the ethene oligomerization in the presence of 3.5NAS catalyst (figure 4) show that higher activity is achieved when the catalyst is activated after heating in vacuum or reduced with CO at temperatures not higher than 673 K. Complete conversion of ethane, mainly to butene and hexane, has been reported by Zhang *et al.* [7] in the case of the thermoactivated 1.7NAS-Ex catalyst. This catalyst exhibits stable activity if the process occurs at temperatures at or below 298 K and no deactivation has been observed. The data on CO adsorption reveal that the 1.7NAS-Ex catalyst activated in this way contains both Ni^{+} and Ni^{2+} ions (see figure 7(A)). It is important to understand which oxidation state of nickel controls the activity and selectivity of the catalyst. In order to answer this question, we will examine the influence of the sulfate ions on the nature of the Ni^{2+} sites. The detailed analysis of the spectral characteristics of the carbonyl complexes with the cus ions of the sulfated catalysts (figures 3 and 7) shows that the Al^{3+} ions of higher coordinative unsaturation (Al^{3+}–CO band at 2235 cm^{-1}) are inaccessible to CO adsorption. Evidently, these sites of the support participate in the formation of the new Ni^{2+}–SO_4^{2-} sites. Another important observation is that the intensity of the Ni^{2+}–CO band on the catalyst prepared by impregnation with $NiSO_4$ (catalyst 3.5NAS) is approximately two times higher than that on the sulfate-free catalyst (3.5NA) with the same content of Ni^{2+} ions (compare figures 2(A) and 3(A)). This enhancement in the intensity cannot be due to superimposition of the band at 2208 cm^{-1} due to Al^{3+}–CO species because its intensity under the same conditions is much weaker (see figure 1(A)). In addition, the Ni^{2+}–CO band in the case of the sulfated catalyst is blue-shifted by approximately 20 cm^{-1}. These differences can be explained by the assumption that in the sulfated catalyst there are a large number of isolated nickel atoms, whereas in the sulfate-free sample most of the nickel atoms are in a state close to the NiO phase. Indeed, carbonyls formed with isolated Ni^{2+} ions have a ν(CO) stretching mode at about 2200 cm^{-1} [21,33–36].

Different activation procedures result in different activities of the catalysts in the oligomerization of ethene. The sample 3.5NAS activated by oxidative treatment exhibits considerably lower activity, which suggests that reduced nickel ions favor the oligomerization process. On the other hand, the sulfate-free 3.5NA catalyst does not possess significant activity [7] although it contains the highest amount of reduced nickel ions (compare figures 2 and 3). It can be concluded from these facts that isolated Ni^{+} represents the active sites for the oligomerization of ethene. These sites are obtained by thermoactivation at 773 K or by reduction with CO up to 673 K and are predominant in the sulfated catalysts containing larger concentrations of isolated Ni^{2+}. The associated Ni^{2+} ions in the sulfate-free catalyst after the activation (figure 2(A)) produce mainly metallic nickel (carbonyls at 2092 and 1830 cm^{-1}) and to a lesser extent associated Ni^{+} ions (carbonyl band at 2127 cm^{-1}). The importance of the isolated Ni^{2+} ions as precursors of the active sites is demonstrated by the fact that the sulfated sample with low nickel content obtained by ion exchange (0.9NAS-Ex) has comparable activity with that of the 3.5NAS catalyst and the additional loading with nickel does not have a significant effect (figure 9). The preparation of the catalyst by ion exchange results in a greater amount of isolated Ni^{2+} ions due to better dispersion, which gives the possibility of lowering the nickel content.

A very important argument supporting the role of Ni^{+} ions as active sites is the result of CO adsorption on the 1.7NAS-Ex catalyst after the process of ethene oligomerization (figure 8). Only carbonyls due to Ni^{2+} and $Ni^{\delta+}$ are observed, whereas the Ni^{+} ions, originally present in the activated catalyst, are occupied by the oligomerization products and do not produce carbonyls.

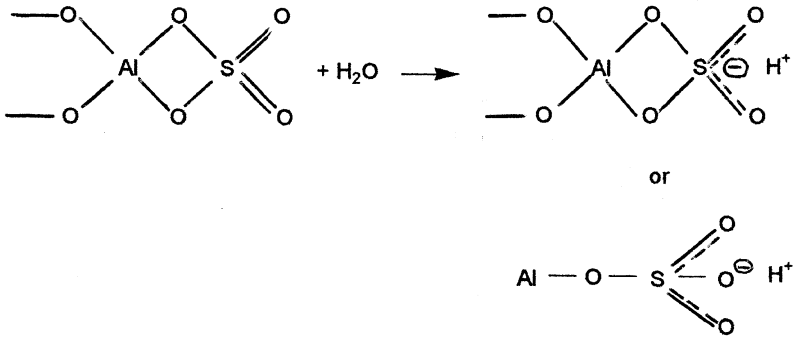

Scheme 1.

The formation of $Ni^{\delta+}$ species indicates that, under contact of the catalyst with the olefin, reduction of Ni^{2+} ions to a low-valence nickel, *e.g.*, $Ni^{\delta+}$ and Ni^{+}, takes place.

It is known that the addition of sulfate ions to alumina leads to the appearance of Brønsted acid sites in contrast to the pure oxide [29,32]. Enhanced Brønsted acidity has been observed after modification of other oxide supports by sulfate ions [37,38]. The experimental data on the 3.5AS and 1.7NAS-Ex samples show that the presence of sulfate ions does not lead to a significant increase in the Lewis acidity (figure 1(C)), but it creates Brønsted acid sites when the sample is not completely dehydroxylated (figure 6). According to the literature data [29,37,38] the appearance of protonic acid sites upon hydration is due to covalently bonded sulfate ions (Scheme 1). We are of the opinion that the latter species are formed by the participation of the basic surface hydroxyl groups of alumina. The concentration of these hydroxyls is not large (0.8 sites/nm^2) [21], which implies low concentration of the covalent sulfates formed. It can be proposed that the proton is delocalized over the oxygen atoms of the SO_3 and SO_2 fragments (Scheme 1), which are at a large distance from each other. This can facilitate the stabilization of isolated nickel ions deposited by ion exchange.

The main difference between the activities of NiO/Al_2O_3 and $NiSO_4/Al_2O_3$ systems in the ethene oligomerization is the presence of quite strong Brønsted acid sites in the latter case. These sites can survive relatively high temperatures of dehydration and they play an important role in the formation of the active sites for ethene oligomerization. It is known that the reduction of Ni^{2+} ions in absence of Brønsted acidity, as in the case of NiO, produces Ni^0 because the oxidation state of Ni^+ is unstable [21]. We believe that the protonic acid sites favor the reduction of Ni^{2+} to Ni^+ ions. In fact, formation of Ni^+ ions has been first established for reduced nickel ions in zeolites where the existence of Brønsted acid sites is not unusual. Here, we observe a similar trend. The reduction of the Ni^{2+} and particularly the isolated Ni^{2+} ions to Ni^+ can occur by recombination of an OH group coordinated to a Ni^{2+} site with a proton from the sulfated support. Another reason for stabilization of nickel ions in the +1 oxidation state could be the existence of isolated Ni^{2+} ions on the catalyst surface. These species can be easily formed by exchange of protons of the sulfated support for nickel(II)-containing ions from the solution. The distances between the exchangeable protons should be large enough to hinder the formation of Ni^{2+} ion clusters on the surface of the sulfated support. Indeed, Espinoza *et al.* [39] have shown that high activity per Ni site can be achieved by selective exchange of nickel ions with sites of high acid strength on a silica–alumina support. It is not surprising that nickel-containing zeolites are among the heterogeneous catalysts reported for the first time to exhibit activity in ethene oligomerization.

5. Conclusions

Isolated Ni^+ ions are the active sites for catalytic oligomerization of ethene on nickel–alumina catalysts modified by sulfate ions. These sites are formed by a reduction process, in which Brønsted acid sites are involved. The modification of the support by sulfate ions favors the dispersion of the precursor Ni^{2+} ions and their reduction to Ni^+ ions.

Acknowledgment

The authors would like to thank to Prof. I.G. Dalla Lana for the offer to perform this investigation in his laboratory at the Department of Chemical and Materials Engineering, University of Alberta, Edmonton, Alberta T6G 2G6, Canada.

References

[1] J. Heveling, C.P. Nicolaides and M.S. Scurrell, Appl. Catal. A 173 (1998) 1.
[2] M.D. Heydenrych, C.P. Nicolaides and M.S. Scurrell, J. Catal. 197 (2001) 49.
[3] Y. Chauvin, D.C. Commeruc, F. Huges and J. Thivolle-Cazal, Appl. Catal. 42 (1988) 205.

[4] F. Huges, D.C. Commeruc, Y. Chauvin, L. Saussine and J.P. Bournonville, French Patent FR 2 641 477, 13 July, 1990.
[5] T. Cai, D. Cao, Z. Song and L. Li, Appl. Catal. A 95 (1993) L1.
[6] T. Cai, Catal. Today, 51 (1999) 153.
[7] Q. Zhang, M. Kantcheva and I.G. Dalla Lana, Ind. Eng. Chem. Res. 36 (1997) 3433.
[8] Q. Zhang and I.G. Dalla Lana, Chem. Eng. Sci. 52 (1997) 4187.
[9] T. Yashima, Y. Ushida, M. Ebisawa and N. Hara, J. Catal. 36 (1975) 320.
[10] G. Wendt, J. Finster, R. Schoellner and H. Siegel, Stud. Surf. Sci. Catal. 7 (1981) 978.
[11] I.E. Elev, B.N. Shelimov and V.B. Kazansky, Kinet. Katal. 23 (1982) 936.
[12] V.B. Kazansky, I.V. Elev and B.N. Shelimov, J. Mol. Catal. 21 (1983) 265.
[13] I.E. Elev, B.N. Shelimov and V.B. Kazansky, J. Catal. 89 (1984) 470.
[14] (a) L. Bonnevoit, D. Olivier and M. Che, J. Mol. Catal. 21 (1983) 415; (b) L. Bonnevoit, O.Legende, M.Kermarec, D. Olivier and M. Che, J. Coll. Interf. Sci. 134 (1994) 534; (c) M. Kermarec, D. Delafosse and M. Che, J. Chem. Soc. Chem. Commun. (1983) 411.
[15] M. Kermarec, D. Olivier, M. Richard and M. Che, J. Phys. Chem. 86 (1982) 2818.
[16] M. Kermarec, C. Lepetit F.X. Cai and D. Olivier, J. Chem. Soc. Faraday Trans. I, 85 (1989) 1991.
[17] A.M. Aljarallah, J.A. Anabtawi, A.A.B. Siddiqui, A.M. Aitani and A.W. Alsadoun, Catal. Today, 14 (1992) 1.
[18] J. Skupinska, Chem. Rev. 91 (1991) 613.
[19] (a) L.B. Orlova, Yu. A. Lokhov, K.G. Ione and A.A. Davydov, Bull. Akad. Nauk SSSR, Ser. Khim. 9 (1979) 93; (b) K.G. Ione, V.N. Romannikov, A.A. Davydov and L.B. Orlova, J. Catal. 57 (1979) 126; (c) E. Garbovski, M.V. Mathieu and M. Primet, Chem. Phys. Lett. 49 (1977) 247.
[20] J.B. Peri, J. Catal. 86 (1984) 84.
[21] A.A. Davydov, *Infrared Spectroscopy of Adsorbed Species on the Surface of Transition Metal Oxides* (Wiley, 1990).
[22] L. Kubelkova, J. Novakova, N.I. Jaeger and G. Schulz-Ekloff, Appl. Catal. A, 95 (1993) 87.
[23] J. Novakova, L. Kubelkova, T. Juska and T. Dolejsek, Zeolite 2 (1982) 17.
[24] P.H. Kasai, J.R. Bishop Jr. and D.J. McLeod, Jr., J. Phys. Chem. 82 (1978) 279.
[25] P.S. Bratermann, *Metal Carbonyl Spectra* (Academic Press, London, 1975).
[26] K. Hadjiivanov, D. Klissurski, M. Kantcheva and A. Davydov, J. Chem. Soc. Faraday Trans. 87 (1991) 907.
[27] H. Knözinger, P. Ratnasamy, Catal. Rev.-Sci. Eng. 17 (1978) 31.
[28] Yu. A. Lokhov and A.A. Davydov, Kinet. Katal. 21 (1990) 1523.
[29] O. Saur, M. Bensitel, A.B. Mohamed Saad, J.C. Lavaley, C.P. Tripp and B.A. Morrow, J. Catal. 99 (1986) 104.
[30] M. Bensitel, O. Saur, J.C. Lavaley and B.A. Morrow, Marer. Chem. Phys. 19 (1988) 47.
[31] E. Laperdix, A. Sahibed-dine, G. Costentin, O. Saur, M. Bensitel, C. Nédez, A.B. Mohamed Saad and J.C. Lavalley, Appl. Catal. B 26 (2000) 71.
[32] W. Pryzystajko, R. Fiedorow and I.G. Dalla Lana, Appl. Catal. 15 (1985) 265.
[33] N.N. Bobrov, G.K. Boreskov, A.A. Davydov and K.G. Ione, Bull. Akad. Nauk SSSR, Ser. Khim. 1 (1975) 24.
[34] V.F. Anufrienko, N.G. Maksimov, V.G. Shinkarenko, A.A. Davydov, *Application of Zeolites in Catalysis* (Nauka, Novosibirsk, 1977).
[35] K.G. Ione, N.N. Bobrov and A.A. Davydov, Kinet. Katal. 16 (1975) 1234.
[36] K.G. Ione, V.N. Romannikov and A.A. Davydov, J. Catal. 7 (1979) 126.
[37] K.I. Hadjiivanov and A.A. Davydov, Kinet. Katal. 29 (1988) 40.
[38] T. Jin, T. Yamaguchi and K. Tanabe, J. Phys. Chem. 90 (1986) 4794.
[39] R.L. Espinoza, C.J. Korf, C.P. Nicolaides and R. Snel, Appl. Catal. 29 (1987) 175.